

Creep deformation cracking of polyethylene in methanol

D. M. SHINOZAKI, R. HOWE

Faculty of Engineering Science, The University of Western Ontario, London, Ontario N6A 5B9, Canada

Compression-moulded high-density polyethylene with a large spherulite size was deformed in methanol, an environment cracking agent. The mechanical test involved constant load creep in tension. At smaller loads corresponding to longer lifetimes, the final failure consisted of a macroscopic crack oriented perpendicular to the tensile axis. Deformed specimens were etched in permanganic acid and the spherulitic and lamellar structures near the macroscopic crack were examined using optical, scanning electron and transmission electron microscopy. The large-scale fracture was the result of crack nucleation in the interlamellar regions and subsequent sub-critical crack growth with micro-cracks joining up to form larger cracks.

1. Introduction

There has been extensive work over the years on the mechanisms of failure in polyethylene (PE), especially as this material became used more in critical load-bearing applications. For example PE pipe is used to transport gases or liquids under pressure, and failure in these cases is related to fracture [1]. In some environments the fracture process is enhanced and the stress to cause failure is lower than that in air [2]. The mechanism involved is one of environmental stress cracking (ESC) occurring at stresses below the gross yield stress of the material. Whereas there is a considerable body of literature on microstructural mechanisms of plastic deformation in air at moderately fast strain rates (corresponding to the familiar tensile test) there is relatively little on ESC at slow strain rates typical of creep tests. In many materials, the mechanisms of deformation change with conditions of testing, even in tension.

Macroscopically, ESC manifests itself as a highly localized, low-ductility fracture which is distinct from the necking and cold drawing seen in PE in air at room temperature. Some evidence for interlamellar failure in ESC of PE has been reported using microstructural observations of fracture surfaces in a scanning electron microscope (SEM) [3, 4]. A theoretical model based on stress-induced swelling and plasticization of the amorphous region has been proposed to explain the observations [5]. A related phenomenon which has been investigated recently is that of crazing in PE [6]. From this work it appears that the intrinsic brittle fracture stress is dependent on the density of tie molecules; that is on the strength of the interlamellar regions. Microstructural studies of morphological changes near sharp notches in PE deformed in tension suggested that micropores are generated in the early stages of deformation [7]. The permanganic etching method outlined by Bassett and Hodge [8] was used to examine the microstructural changes around the notch tip. However, Battacharya and Brown [7] found

that the etched microstructure was obscured by artifacts produced by the etching process. These nodular artefacts had been reported previously by Olley and Bassett [9]. The process of permanganic etching of PE has been further examined by Naylor and Phillips [10] and the variously shaped artefacts, both nodular and star-shaped have been shown to nucleate near surface scratches. It is therefore of some interest to apply this etching technique to the study of ESC in PE, taking suitable precautions to eliminate artifacts.

The advantages of using permanganic etching compared to previous work on mechanisms of deformation are, (i) lamellar morphologies are revealed, and (ii) bulk material may be examined. Earlier TEM and optical examination studies of deformation largely have been limited to thin film specimens [11-14]. The thickness of the mechanically tested specimen is significant since spherulitic solids are elastically and plastically inhomogeneous. Mechanisms of ESC or spherulitic deformation, for example the cavitation proposed by Brown *et al.* [7], are affected by the state of stress which, in turn, depends on the plastic constraint. The ECS crack nucleation process also likely initiates at the specimen surface. Thus studies of etched, deformed bulk specimens are necessary.

2. Experimental procedure

Two forms of PE were used; a Dupont Sclair resin and an uncharacterized commercial sheet of HDPE. The Sclair resin was supplied by Peter Kelly of Dupont Canada and had a 65% crystallinity (measured with a laser Raman technique); a molecular weight of $M_n = 17\,800$ and $M_w = 61\,500$ (GPC). It was compression moulded and tensile specimens cut from the sheets with a gauge length of dimensions $3.5\text{ cm} \times 0.4\text{ cm} \times 0.3\text{ cm}$.

The mechanical test was a constant load machine with a gripping arrangement to allow the specimen to be immersed in methanol. Evaporation of the methanol cooled the insulated bath of 14°C , at which

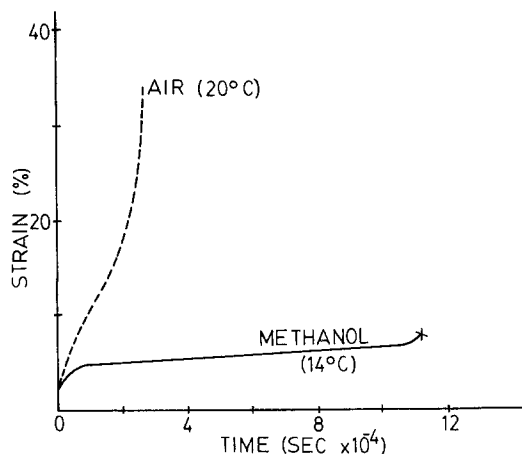


Figure 1 Typical tensile creep curves for Sclair PE at an applied stress of 14 MPa.

temperature the tests were run. The elongation of the specimen was measured as a function of time using a linear variable displacement transducer. Constant load creep tests were run at a variety of loads in air and in methanol to give lifetimes of 3 to 40 h.

The uncharacterized sheet and Sclair PE were etched using the general methodology of Bassett *et al.* [15] with some changes to minimize artefact formation. The Sclair resin revealed a clearer lamellar morphology than did the uncharacterized sheet. Optical sections cut from the centre of the air-deformed specimen confirmed that spherulite shape changes were similar to those seen in the etched spherulites on the surface. The results presented here are of structures seen on the surface of the specimens.

The microstructures were examined with reflected light; with scanning electron microscopy (SEM) in an ISI DS130; and with transmission electron microscopy (TEM) of two stage cellulose acetate/AuPd shadowed carbon replicas in an Hitachi H800, amongst other instruments.

3. Results

In the compression-moulded state, the Sclair PE consisted of a banded spherulite structure with a band separation between 2 to 4 μm . The typical spherulite diameter was in the range 50 to 100 μm . The uncharacterized PE had no clear spherulite structure.

Examples of creep curves obtained for this material deformed in air and in methanol are shown in Fig. 1. The ultimate failure under these conditions consisted of necking and drawing in air and low ductility fracture in methanol. The gross fracture plane in methanol was normal to the applied tensile axis and no necking was observed. However, at stresses higher than shown in Fig. 1, the specimen necked appreciably before fracture. The microstructural observations on ESC deformation described here are therefore taken from specimens deformed in methanol at relatively low stresses, in which the gross failure mode is similar to that reported for ESC. The creep tests in methanol were stopped at or near failure, at which point large cracks were visible in the specimen, as seen in Fig. 2. This shows a crack in uncharacterized PE, and is similar to the cracks seen in Sclair PE. Both materials showed smaller cracks finely distributed over the gauge length of the specimen, particularly near the large cracks. These were visible before and after

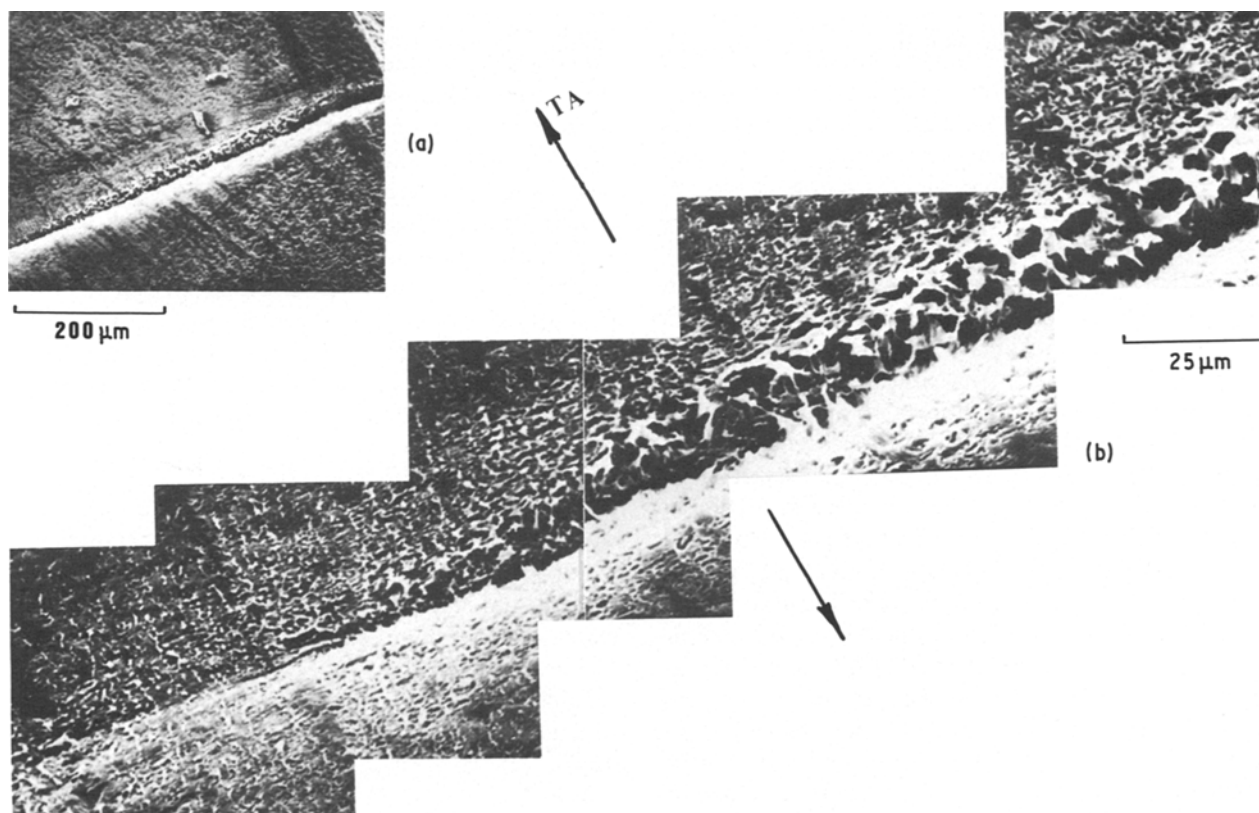


Figure 2 Methanol-induced crack in uncharacterized PE (a) at low magnification and (b) at higher magnification. Permanganic etched and viewed in an SEM.

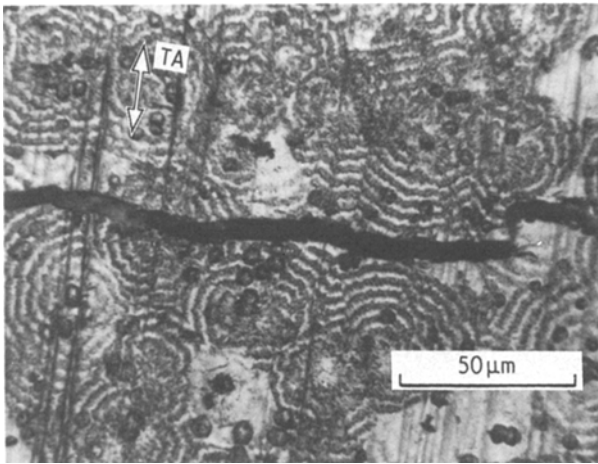


Figure 3 Sclair PE deformed in methanol. Viewed in reflected light.

permanganic etching and are therefore not an artefact of the chemical process of etching.

The large cracks, and in the case of fractured specimens the fracture plane, did not follow any recognizable microstructural path over most of their length. However, examination of the smaller sub-critical cracks revealed the influence of local microstructure on methanol enhanced cracking. In Fig. 3, medium sized cracks are clearly not continuous, and appear to run along spherulite boundaries and centres. Finer cracks seen in Fig. 4 confirm this. In other areas of the specimen, the local crack plane occasionally deviates from the plane normal to the tensile stress to follow spherulite radial directions (as in Fig. 5 and in Fig. 6). Independently initiated cracks lengthen and join up along paths of weakness through spherulites and at their boundaries (Fig. 7). The ultimate failure likely occurs as number of these finer cracks join up to form a critical crack length which propagates rapidly through the remaining specimen section.

The smallest cracks observed in the TEM replicas (Figs. 8 and 9) suggest that the earliest nuclei are in the interlamellar regions and are of the order of 10 nm wide, and as long as the local lamella, perhaps 1 to 10 μm. These micrographs have been compared to identically prepared, undeformed specimens, and to specimens deformed in creep in air. These cracks appear only after deformation in methanol at relatively

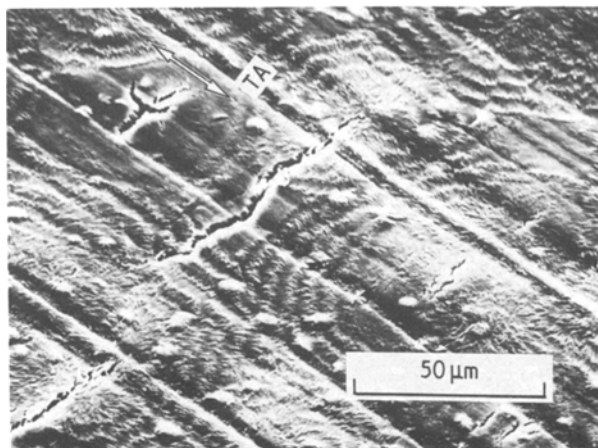


Figure 4 Cracks at spherulite centres and boundaries (SEM).

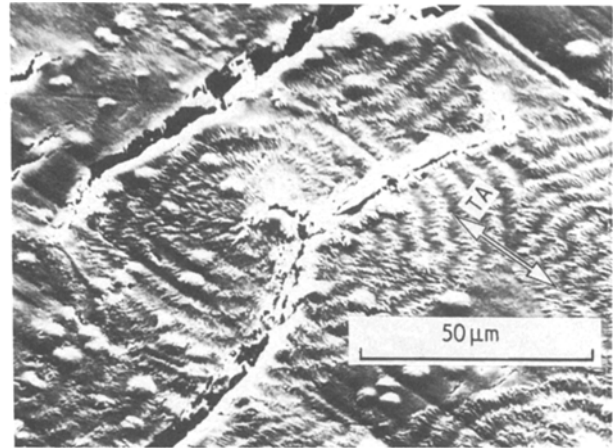


Figure 5 Propagation of cracks in radial direction through a spherulite (SEM).

low stresses in creep and therefore are a manifestation of ESC crack nucleation.

4. Discussion

Microstructures observed using the permanganic etching technique are similar to those seen by others and artefacts produced on etching are clearly distinguishable from the true microstructure of PE. The cracks seen in the Sclair PE creep tested in methanol are deformation structures since they are seen before and after etching. The smallest cracks seen in the surface of the deformed specimen are of the order of 10 nm wide in the interlamellar regions. The relatively larger cracks seen optically or in the SEM are evidently produced when the interlamellar cracks grow, and join up. The final, gross ESC fracture plane is normal to the tensile axis, but the crack nuclei are found at orientations which are not necessarily in this plane. The ESC fracture process then appears to consist of a microcrack nucleation step, followed by a macroscopic fast fracture.

The micro-crack nucleation in the interlamellar regions might occur in two ways. Firstly, they may be a result of interlamellar separation as in a Mode I crack opening under a maximum normal stress. The equatorial regions of the spherulite would contain the interlamellar planes oriented approximately in this plane. The cracks at the spherulite boundaries may

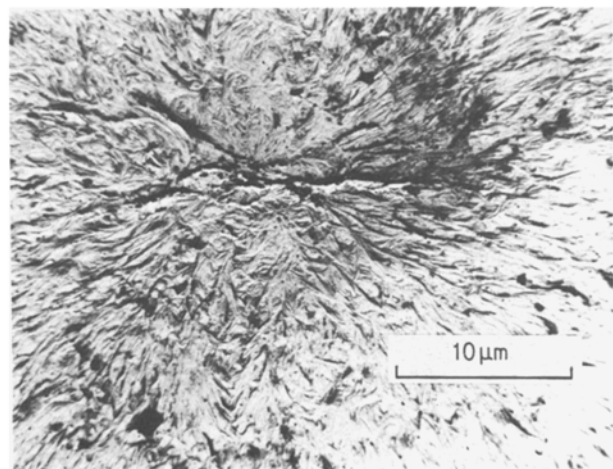


Figure 6 TEM view of radial cracks.

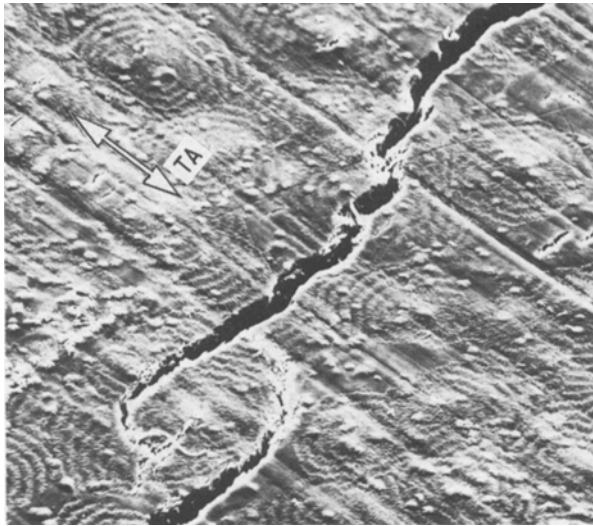


Figure 7 Interaction of cracks propagating through the spherulites. (1 cm = 50 μm .)

be due to the inherent weakness of the boundary. However, similar cracks have not been found in PE deformed in creep in air unless the specimen is etched in the permanganic acid. Air-deformed Sclair PE shows no sharp interlamellar cracks but rather equiaxed voids which appear after permanganic etching. Such voids are sometimes found in the spherulite boundary regions in the boundaries perpendicular to the tensile axis. This suggests that the region may not be inherently weak but may be a region of residual stress which preferentially etches due to the stored stress.

The reason this may be a region of high internal stress in a deformed material is that the equatorial sectors plastically deform before the polar sectors (Fig. 10). The plastic contraction of the equatorial sectors can induce a hydrostatic tension on the polar sectors, thereby increasing the tendency to crack or cavitate in these regions.

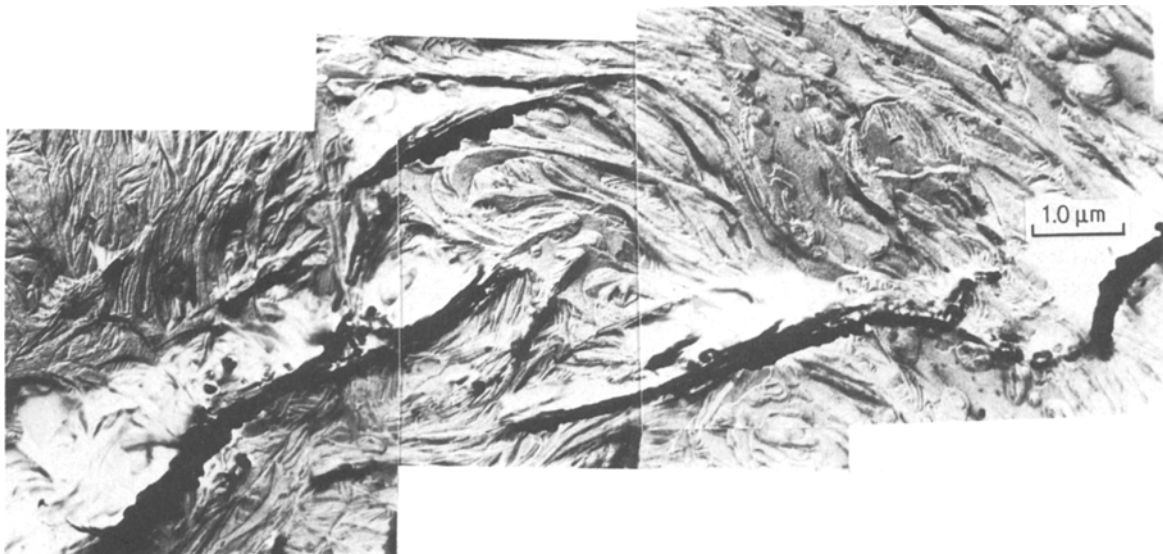


Figure 8 TEM image of interlamellar cracks.

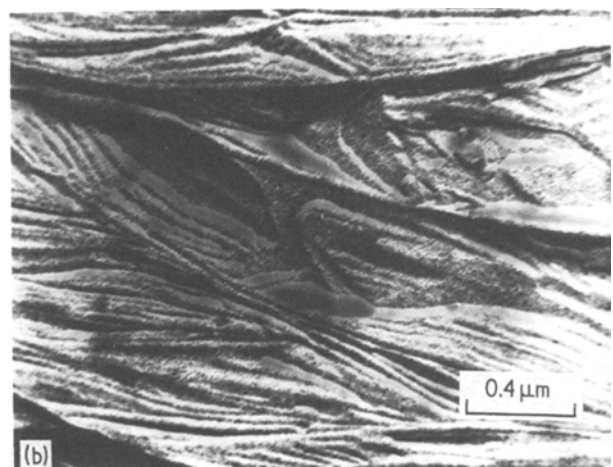
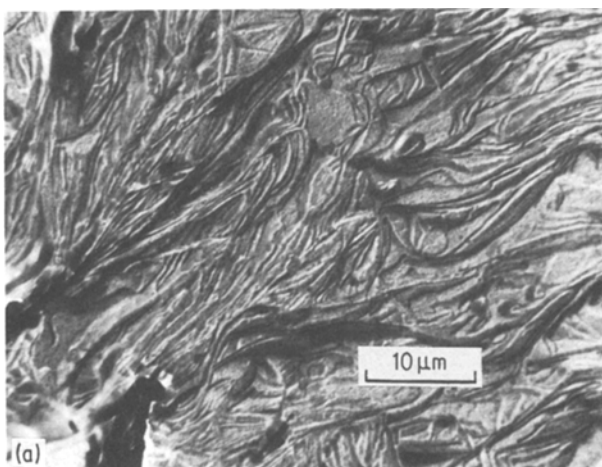


Figure 9 (a) and (b) TEM images of fine interlamellar cracks.

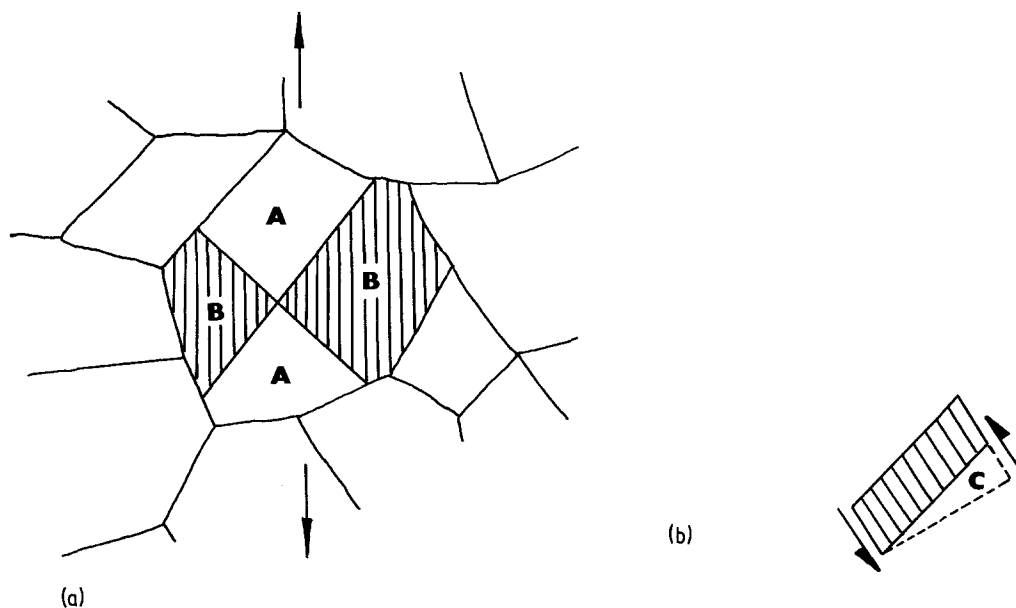


Figure 10 (a) Generation of hydrostatic tension in the polar sections (A) of spherulites due to the plastic deformation in the equatorial regions (B). (b) Interlamellar cracks (C) resulting from intermolecular slip in lamellae.

An alternative mechanism to produce interlamellar cracks is the breakdown of compatibility at the crystallite boundaries (Fig. 10b). The critical resolved shear stress for intermolecular slip is small [16], and some local slip may be expected for those lamellae with the highest resolved shear stress on the intermolecular system. The limited number of slip systems in the PE crystal means that any slip in one lamella will not necessarily be accommodated by slip in a neighbouring lamella with a different orientation. The boundary then opens out as a crack in a way analogous to interface cracking at the head of dislocation pile-ups in other materials [17]. In tensile testing of PE at higher strain rates, this kind of cracking may be masked by generalized plastic flow occurring at the higher applied stresses. However, macroscopic plastic volume changes in tensile-tested PE show there exists some plastic dilation of the structure [18]. The role of the ESC agent such as methanol is likely to reduce the surface energy to lower the critical stress necessary to open the crack in the interlamellar region. This agrees with the work of Kamei and Brown [6]. However, there is no evidence to support the presence of micropores in the region of the macroscopic ESC crack path, as have been observed by Battacharya and Brown in air deformed, notched PE [7]. Such micropores may exist under load and disappear when unloaded, or it is possible relatively high strain rates are required to produce these micropores.

Once the crack nuclei are formed between lamellae, they extend and join other cracks, and the resultant crack plane is not necessarily planar, as material between the microcracks is drawn out. Once the crack is long enough, and the stress at the crack tip large enough, the crack propagates rapidly through the microstructure without following the interlamellar regions, simply propagating on a plane perpendicular to the applied stress. This would explain the similar macroscopic deformation behaviour of spherulitic and non-spherulitic and non-spherulitic PE.

5. Conclusions

The permanganic etching has been used to examine deformation of PE in creep in methanol, an environmental crack agent. Large cracks or crazes appear in the spherulite's centres and boundaries, on planes approximately normal to the applied tensile stress. Careful high-resolution examination reveals small, interlamellar cracks less than 10 nm wide which apparently join up to form the larger trans-spherulite and interspherulitic cracks. Some models based on inhomogeneous slip and plasticity are suggested to account for the observations.

Acknowledgements

The experiments were supported by an NSERC (Canada) operating grant. Other aid was obtained from MRC (Canada), and the Centre for Chemical Physics at the University of Western Ontario. Peter Kelly of Dupont supplied the material and Don Gibson of the Department of Pathology kindly helped in the TEM studies.

References

1. M. B. BARBER, J. BOWMAN and M. BEVIS, *J. Mater. Sci.* **18** (1983) 1095.
2. M. E. R. SHANAHAN and J. SCHULTZ, *J. Polym. Sci. Phys.* **18** (1980) 19.
3. S. BANDYOPADHYAY and H. R. BROWN, *J. Mater. Sci.* **12** (1977) 2131.
4. *Idem*, *Polymer* **19** (1978) 589.
5. H. R. BROWN, *ibid.* **19** (1978) 1186.
6. E. KAMEI and N. BROWN, *J. Polym. Sci. Phys.* **22** (1984) 543.
7. S. K. BHATTACHARYA and N. BROWN, *J. Mater. Sci.* **19** (1984) 2579.
8. D. C. BASSETT and A. M. HODGE, *Proc. R. Soc. A* **377** (1981) 25.
9. R. H. OLLEY and D. C. BASSETT, *Polymer* **23** (1982) 1707.
10. K. L. NAYLOR and P. J. PHILLIPS, *J. Polym. Sci. Phys.* **21** (1983) 2011.
11. D. E. MOREL and D. T. GRUBB, *Polymer* **25** (1984) 417.

12. P. M. TARIN and E. L. THOMAS, *Polym. Eng. Sci.* **18** (1978) 472.
13. J. L. WAY and J. R. ATKINSON, *J. Mater. Sci.* **6** (1971) 102.
14. E. WEYNANT, J. M. HAUDIN and G. S'ELL, *ibid.* **15** (1980) 2677.
15. D. C. BASSETT, A. M. HODGE and R. H. OLLEY, *Proc. R. Soc.* **15** (1980) 2677.
16. R. J. YOUNG, "Introduction to Polymers" (Chapman and Hall, London, 1981).
17. A. KELLY and G. W. GROVES, "Crystallography and Crystal Defects" (Addison-Wesley, London, 1970).
18. W. A. SPITZIG and O. RICHMOND, *Polym. Eng. Sci.* **19** (1979) 1129.

*Received 15 January
and accepted 11 July 1985*